Comparative analysis reveals gravity is involved in the MIZ1-regulated root hydrotropism

Ying Li[1, #], Wei Yuan[1, #], Luocheng Li[1], Hui Dai[1], Xiaolin Dang[1], Rui Miao[1], František Baluška[2], Herbert J. Kronzucker[3,4], Congming Lu[5], Jianhua Zhang[6], Weifeng Xu[1,*]

[1]Center for Plant Water-use and Nutrition Regulation and College of Life Sciences, Joint International Research Laboratory of Water and Nutrient in Crop, Fujian Agriculture and Forestry University, Jinshan Fuzhou 350002, China

[2]Institute of Cellular and Molecular Botany, University of Bonn, 53115 Bonn, Germany

[3]School of Agriculture and Food, Faculty of Veterinary and Agricultural Sciences, The University of Melbourne, VIC 3010, Australia

[4]Faculty of Land and Food Systems, University of British Columbia, Vancouver, BC V6T 1Z4, Canada

[5]State Key Laboratory of Crop Biology, College of Life Sciences, Shandong Agricultural University, Taian, Shandong 271018, China

[6]Department of Biology, Hong Kong Baptist University, Stake Key Laboratory of Agrobiotechnology and Chinese University of Hong Kong, Hong Kong

[#] These authors contribute equally to this work.

*** Corresponding author:**

Weifeng Xu, Tel: + 86 591 83737535; E-mail: wfxu@fafu.edu.cn;

E-mail address of each author:

Ying Li: 1372468861@qq.com; Wei Yuan: 292547026@qq.com; Luocheng Li, 545485954@qq.com; Hui Dai: 970528304@qq.com; Rui Miao: miaorui2011@126.com; Xiaolin Dang: 1157833534@qq.com; František Baluška: unb15e@uni-bonn.de; Congming Lu: cmlu@sdau.edu.cn; Herbert J. Kronzucker: herbert.kronzucker@unimelb.edu.au; Jianhua Zhang: jzhang@hkbu.edu.hk.

Highlight

The divergent roles of gravity in root hydrotropism contribute to the acquisition of water from different directions in a heterogeneous soil environment.

Abstract

Hydrotropism is the directed growth of roots toward the water found in the soil. However, mechanisms governing interactions between hydrotropism and gravitropism remain largely unclear. In this study, we found that air-system and agar-sorbitol-system only induced oblique water-potential gradients; agar-glycerol-system only induced vertical water-potential gradients; sand-system established both oblique and vertical the water-potential gradients. We employed obliquely-oriented and vertically-oriented experimental systems to study hydrotropism in *Arabidopsis* and tomato plants. We found that the gravitropism-deficient mutant *aux1* showed enhanced hydrotropism in the oblique orientation but impaired root elongation towards the water in a vertical orientation. *Miz1* mutant exhibited deficient hydrotropism in the oblique orientation but normal root elongation towards the water in a vertical orientation. We performed comparative analyses using different hydrotropic systems and found that gravity hindered the ability of roots to search for obliquely-oriented water. Importantly, in contrast to *miz1*, the *miz1/aux1* double-mutant exhibited hydrotropic bending in the oblique orientation. Additionally, gravity facilitated roots' search for vertically-oriented water, because the *miz1/aux1* double-mutant showed attenuated root elongation towards the water in a vertical orientation, in contrast to *miz1*. Our results suggest that gravitropism is required for MIZ1-regulated root hydrotropism in both the oblique orientation and vertical orientation, providing further insight into the role of gravity in root hydrotropism.

Keywords: Arabidopsis; gravitropism; hydrotropism; *MIZ1*; root; water-potential

Abbreviations: Obliquely oriented hydrotropic experimental system (OHES); Sand system for oblique orientation hydrotropism (SSO); Sand system for vertical orientation hydrotropism (SSV); vertically oriented hydrotropic experimental system (VHES).

Introduction

Because plants are sessile organisms, plant growth and development display exceptional plasticity, allowing for rapid acclimation to a changing environment (Zhu, 2016; Dietrich *et al*., 2017; Su *et al*., 2017; Shkolnik *et al*., 2018). One such acclimation response is tropism, which is the directed growth of plant tissues in response to various stimuli, including gravity, light, temperature, oxygen, touch, and water (Silva-Navas *et al*., 2016; Eysholdt-Derzso and Sauter, 2017; Dietrich, 2018; Vandenbrink and Kiss, 2019; Muthert *et al*., 2020). Among these is hydrotropism, the directed growth of roots in response to water potential gradients, which can help plants overcome the detrimental effects of drought (Eapen *et al*., 2003; Kobayashi *et al*., 2007; Lynch, 2013; Eapen *et al*., 2017). However, there have been few studies on hydrotropism in much of the last century because of the difficulty designing experimental systems that can reproducibly simulate the water potential gradients found in soils and the simultaneous effect of gravity on directing root growth (Takahashi and Scott, 1991; Stinemetz *et al*., 1996; Kiss, 2007; Takahashi *et al*., 2009).

A classic hydrotropism system to examine the hydrotropic response of roots was first used by Sachs (Sachs, 1872); this system involved placing a few plant seeds in a hanging cylinder of wet sawdust held together by a mesh screen, resulting in root growth toward the wet substratum exhibiting true hydrotropism. Using Julius Sachs' experimental system, Darwin indicated that water potential gradients influenced directional root growth in *Phaseolus*, *Vicia*, *Avena*, and *Triticum* (Darwin and Darwin, 1880; Hooker, 1915). More modern systems to examine hydrotropism in *Arabidopsis* have been developed by two groups, who used the systems to isolate hydrotropism mutants (Takahashi *et al*., 2002; Eapen *et al*., 2005). Takahashi *et al*. (2002) developed obliquely oriented hydrotropic experimental systems (OHESs), including an air system and an agar-sorbitol system, and identified the no-hydrotropic mutant *miz1* (Kobayashi *et al*., 2007). These screening systems also led to the isolation of *miz2* mutant, which is deficient in the *GNOM* gene (Miyazawa *et al*., 2008). In another approach, Saucedo *et al*. (2012) developed vertically oriented hydrotropic experimental systems (VHESs), including an agar-glycerol system, and isolated a mutant with altered hydrotropic responses (*ahr1*). To date, however, the genetic locus of *AHR1* has not been identified (Saucedo *et al*., 2012). In addition, although Cole and Mahall (2006) developed a sand-based system for analyses of root hydrotropism in dune shrubs, there was no compelling evidence for hydrotropic root growth. Iwata *et al*. (2013) studied hydrotropism

in *Arabidopsis* under natural conditions using an image scanner. However, the investigation of root hydrotropism using the natural drought system is challenging, and the operating procedures may be impractical, especially cumbersome. Thus, the development of an improved system that accurately simulates natural conditions is essential for the elucidation of the mechanisms underlying hydrotropic responses.

Previous studies have reported that gravitropism might interact with hydrotropism to influence the direction of the growth of roots (Jaffe *et al*., 1985; Takahashi *et al*., 2003; Takahashi *et al*., 2009). Consequently, agravitropic mutants, clinorotation, and space experiments with plants (microgravity in space) have been used to differentiate hydrotropic from gravitropic responses (Takahashi *et al*., 1999; Takahashi *et al*., 2003; Takahashi *et al*., 2009; Morohashi *et al*., 2017). *Arabidopsis* roots of the gravitropism-deficient mutant or starchless mutant tend to display a greater hydrotropic response (Chang *et al*., 2019), and anti-auxin reagents enhance the hydrotropic response in *Arabidopsis* roots (Takahashi *et al*., 2009; Krieger *et al*., 2016; Shkolnik *et al*., 2016). Furthermore, the hydrotropism-deficient mutant *miz1* shows reduced phototropism and altered wavy growth responses, suggesting that hydrotropism may interfere with other tropisms in *Arabidopsis* (Simmons *et al*., 1995; Kobayashi *et al*., 2007). However, it has not yet been elucidated how MIZ1-modulated root hydrotropism is influenced by gravitropism, and thus it remains necessary to disentangle the relevance of the two major root tropisms.

In this study, we performed a quantitative survey of the scientific literature on root hydrotropism and assessed to what extent the imperfections in each of the experimental systems used presents challenges to our interpretations of root-tropic responses. Furthermore, we designed an improved sand system to study hydrotropism, in which a realistic water potential gradient is established, not only in the vertical orientation but also in the oblique orientation under natural conditions. Moreover, based on previous systems and our sand system, we used RNA sequencing, cell biology and genetic crossing, we found that gravitropism is important for root hydrotropism. Notably, we found that gravity hinders the ability of roots to search for obliquely oriented water, while it helps their search for vertically oriented water; MIZ1 is involved in these two processes.

Materials and methods

Plant materials and growth conditions

The Col-0 ecotype of *Arabidopsis* (*Arabidopsis thaliana* (L.) Heynh) was used as the wild-type (WT) unless otherwise indicated. Other *Arabidopsis* plants used in the study were previously described: *miz1* and *ahr1* (Miao *et al*., 2018), DR5:GFP (Xu *et al*., 2013a), DII-VENUS (Band *et al*., 2012), and AUX1:YFP lines (Li *et al*., 2011). The *Arabidopsis* mutant *pgm1–1* (CS210) was obtained from the *Arabidopsis* Biological Resource Center. The following gravitropic mutants were used: auxin-influx transporter mutant *aux1–7* (Bennett *et al*., 1996), gravitropism-deficient auxin response factor double-mutant *arf10/arf16* (Wang *et al*., 2005), and starch-deficient mutant *pgm1–1* (Kiss *et al*., 1989), which displays a substantial impairment in gravitropic responses. Seeds were surface sterilised with 1.5% (w/v) NaClO for approximately 15 min, washed 3–5 times with autoclaved water, and stratified at 4°C in the dark for 2 days to break seed dormancy and synchronise germination. Subsequently, the seeds were placed on half-strength Murashige and Skoog (MS) medium (Sigma) supplemented with 1% (w/v) sucrose and 1% (w/v) agar (pH 5.8). Five-day-old uniform seedlings were subsequently transferred and planted vertically in a growth chamber at 22°C–23°C under 100–150 μmol photons·m^{-2}·s^{-1} with a 16 h/8 h light/dark cycle and 60% relative humidity. Tomato (LA0534) seeds were germinated on filter paper at 28°C in the dark.

Root hydrotropism systems

The air system shown in Figs. 1A-C, 4D, and 5E was established as previously described (Takahashi *et al*., 2002). To determine the root hydrotropic bending, we carefully cut off each *Arabidopsis* root grown on agar together with the agar block; the cut agar block with one seedling was photographed using a stereomicroscope and analysed with ImageJ software. The agar-sorbitol system shown in Figs. 1D-F, 4A-C, and 4E was established as previously described (Takahashi *et al*., 2002). To determine the root hydrotropic bending, we photographed the square plates using a digital Nikon camera D7100 and analysed the images using ImageJ. The direction of gravity was considered 0 degrees, and the angle of deviation from the direction of gravity was determined as the hydrotropic angles of roots in both systems (Fig. 1). The agar-glycerol system shown in Fig. 2 was established as previously

described by Eapen *et al*. (2003). Roots were photographed using a digital Nikon camera D7100, and images were analysed using ImageJ to measure the length of roots.

The sand system for oblique orientation hydrotropism (SSO) shown in Figs. 3A-D and 5F consisted of a square plate (10 × 10 × 1.5 cm) filled with sand (approximately 210 g). The sand had previously been passed through a sieve with a 0.8 mm mesh, sifted, and washed 3–5 times with water, followed by autoclaving and drying for two days at 65°C. Six-day-old seedlings grown under normal conditions (half-strength MS medium) were transplanted onto square plates equipped with square holes (1.5 × 1.5 mm, L × W) in the medium plate, and covered with sand taking care not to damage roots; the sand was immediately saturated with approximately 55 mL distilled water (pH 6.3). To maintain a high water content, we fully covered the plate with a lid. To establish experimental water potential gradients, we covered the left half of the plate with sterile gauze; the right half of the plate was sealed with plastic film, which prevented evaporation. To maintain the water content gradient in the hydrostimulated chamber for a relatively long period of time, we supplied 10 mL water only to the right side of the plate through an injection port 5 and 7 days after transplantation. The chambers were held at an angle of 25 degrees from the vertical axis to promote root growth along the transparent bottom side of the plate. Then the device was placed in a growth chamber with a relative humidity of 60% at 22°C.

The sand system for vertical orientation hydrotropism (SSV) shown in Figs. 3E-H and 6 consisted of a polystyrene cup (5 in lower diameter × 6.5 in upper diameter × 8 cm in height for *Arabidopsis*, or 6.5 in lower diameter × 8 in upper diameter × 12 cm in height for tomato), filled with sand and distilled water (pH 6.3). The sand used in the SSV was the same as that used in the SSO described above and was sieved and sterilised. All cups were saturated with distilled water from the bottom of the container. *Arabidopsis* seeds were surface sterilised and sown onto the surface sand layer using a transfer pipette. For all experiments presented here, treatments started 5 or 7 days after sowing (DAS). For each chamber, one of the halves was randomly selected to serve as the "control" and the other as "hydrostimulated." To maintain the sand at a high water content, we immersed the bottom of the cups in distilled water throughout the experiments. To establish experimental water potential gradients along the gravity vector, we withheld water (simulating natural drought) after DAS 7 or 9, so that the water potential of the hydrostimulated chamber in the sand surface gradually decreased due to drainage and evaporation over time, resulting in relatively higher water content in the

deeper sand layers. During hydrotropic growth, the main roots elongated towards the wet sand (sites of higher water potential) at the bottom of the cups following the gravitropic vector. Then the device was placed in a 22°C growth chamber, with a relative humidity of 60%.

Measurement of water content in the sand system

For sand system-based analyses of obliquely oriented water (Fig. 3A, B), the control and hydrostimulated chambers were divided into four zones (I, II, III and IV) from left to right (2.5 cm width for each zone). For vertically oriented water (Fig. 3E, F), the control and hydrostimulated chambers were divided into four zones (I, II, III and IV) from top to bottom (2 cm height for each zone). Each zone was collected carefully with a spoon, and their weights were determined (fresh weight). The dry weights of the sand were also determined after a 48 h incubation at 65°C. The water content was calculated using the following formula:

$$W = \frac{F - D}{F} \times 100\%$$

where W represents the water content, F is the fresh weight, and D is the dry weight (Munne-Bosch and Alegre, 2002).

Raw and pseudo-coloured sand images

For the SSO, the lid covering the control and plastic film/sterile gauze covering the hydrostimulated chamber were removed after hydrostimulation. For the SSV, the cups were carefully cut lengthwise with scissors after hydrostimulation. Raw sand images were taken using a digital Nikon camera D7100. To enhance the visualisation of moisture distribution in the raw sand images, we enhanced the differences in grey-scale intensity values using ImageJ and a 16-colour look-up table (LUT) (Rellan-Alvarez *et al*., 2015). Pseudo-coloured images (Fig. 3B, F) were generated from the raw images (Fig. 3A, E), and water contents were colour-coded using an appropriate LUT. The differences in grey-scale intensity values indicated moisture content gradients. Water contents in the sand were mapped and visualised; low water contents were represented in red, and high water contents were represented in blue (Fig. 3B, F).

Root harvest and phenotypic analyses in the sand system

The gauze and plastic film in the SSO system were removed using scissors, and the sand was removed from the plates by rinsing carefully with water. After all of the sand was removed, wet roots along the bottom side of the plate were covered with a dry filter paper taking care to leave the root structure undisturbed; the filter paper and all of the roots attached to it were carefully transferred onto the bench with tweezers and photographed with a digital Nikon camera D7100. For each root sampling, we extracted the root systems by hand. The cups in the SSV were cut along both sides with scissors, followed by rinsing with water. Seedlings were clamped with tweezers, and sand was removed from roots by shaking carefully. Seedlings were photographed using a digital Nikon camera D7100.

Primary root length analyses

The height of the cup in the SSV system was 8 cm; the top of the cup was considered 0 cm deep. To determine the length of the primary root, we cut the cup lengthwise with scissors; after rinsing with water, the sand was removed from the roots by shaking carefully. To minimise the influence of inherently shorter roots (e.g., some gravitropism mutants), we used the relative primary root length. The primary root length of control plants was considered 100%, and the relative primary root length was calculated based on the primary root length relative to the displacement of the primary root apex for the duration of hydrostimulation, as described previously (Xu *et al*., 2013).

RNA sequencing and data analyses

Because the hydrotropic angles of wild-type roots in oblique agar-sorbitol systems are approximately 30 degrees 12 h after the start of hydrostimulation, we obtained root samples 10 h after the start of hydrostimulation. Approximately 0.2 g whole root tissues were harvested. The harvested roots were immediately frozen in liquid nitrogen and stored at -80°C. Three biological replicate samples were collected. For RNA sequencing, total RNA was extracted from roots according to the method described by Miao *et al*. (2018). The quality and quantity of the total RNA were assessed using the 2100 Bioanalyzer instrument (Agilent Technologies, Santa Clara, CA, USA). First-strand cDNA was synthesised using the First-Strand cDNA Synthesis Kit (Roche) according to the manufacturer's instructions. Sequencing was performed using the BGISEQ-500 sequencer (BGI, Shenzhen, China).

Data processing of RNA-Seq experiments raw data in the fastq format was first processed by SOAPnuke (version 1.5.2). Clean data were obtained by removing reads containing adapter, poly-N and low-quality reads from raw data. The remaining high-quality reads were mapped against the *Arabidopsis* Information Resource reference genome (TAIR10) using HISAT2 (version 2.1.0). To determine transcript abundance, we calculated the values of fragments per kilobase of transcript per million mapped fragments (FPKM) using Bowtie2 (Version2.2.5). Differential gene expression analyses were carried out using DEGseq. For each pairwise comparison, genes with $\log_2$ (fold change) > 1.5 or <-0.5 and false discovery rate (FDR) < 0.05 were considered differentially expressed genes (DEGs). Gene annotations were obtained from TAIR. Colour-coded gene expression was visualised using the Heatmapper (http://www2.heatmapper.ca/expression/).

Confocal microscopy

The fluorescence of DR5:GFP, DII-VENUS, and AUX1:YFP in *Arabidopsis* root tips was observed with a Zeiss LSM 780 laser spectral scanning confocal microscope as described by Xu *et al*. (2013b). For DR5:GFP, excitation at 488 nm and emission at 510–540 nm were used; for VENUS, excitation at 488 nm and emission at 520–570 nm; and for YFP, excitation at 514 nm and emission at 530–550 nm were used. Roots were stained with a solution of 25 μM propidium iodide (PI) in water for 2 min and rinsed prior to imaging. PI was excited at 552 nm and detected at 600–700 nm. Signal intensity was quantified as the mean grey value using the open-source software ImageJ. Approximately 10 seedlings were imaged per group, and at least two independent experiments were performed. All images were taken under identical conditions.

Starch staining and light microscopy

Amyloplast is a starch-containing non-coloured plastid. Measurement and observation of amyloplasts in the columella cells of the root caps were performed by staining with iodine/potassium iodide solution, as previously described by Takahashi *et al*. (2003).

Statistical analyses

All statistical tests and error bars are described in the figure legends. All statistical analyses were carried out using SPSS, version 17.0. For comparison between two groups, the two-tailed Student's *t*-test was used. *P*-values < 0.05 were considered statistically significant. For

comparisons between more than two groups, Duncan's test with an alpha level of 0.05 was used.

Results

Single-orientation hydrotropism systems are commonly used to investigate root hydrotropism in *Arabidopsis*

To assess how many and which hydrotropism systems have been used in previous studies, PubMed Central open-access full-text articles were screened for keywords related to hydrotropism in *Arabidopsis* (Claeys *et al*., 2014). As shown in Supplementary Fig. S1, two types of system have been commonly used to study root hydrotropism in *Arabidopsis*: OHESs, including air systems (Takahashi *et al*., 2002; Noriega-Calixto *et al*., 2019), agar-sorbitol systems (Takahashi *et al*., 2002), and natural drought systems (Iwata *et al*., 2013); and VHESs, commonly using agar-glycerol systems (Miao *et al*., 2018). Air systems were used in 68% of the studies, while agar-sorbitol, agar-glycerol, and natural drought systems were used in 36%, 24%, and 4% of studies, respectively (Supplementary Fig. S1). The vast majority of studies employed single-orientation hydrotropism systems (88%), whereas agar-glycerol systems and OHESs were used in only 12% of the studies (Supplementary Fig. S1).

The hydrotropic response induces oblique root orientation in air systems and agar-sorbitol systems

Air and agar-sorbitol systems were the first systems used to study root hydrotropism in *Arabidopsis* (Takahashi *et al*., 2002). In this study, we employed both to evaluate the hydrotropic response of *Arabidopsis* roots (Fig. 1A, D). *Arabidopsis* (wild-type, Col-0) roots bent towards the wet agar and deviated from the gravity vector in the hydrostimulated chamber (Fig. 1B, E), while wild-type root growth followed the gravity vector and did not display bending toward the agar in the control chamber (Fig. 1C, F). As expected, *miz1* root growth followed the gravity vector and did not bend toward water-rich agar (Fig. 1B, E), confirming the previously described performance of the two hydrotropic experimental systems (Kobayashi *et al*., 2007). Next, we compared the hydrotropic responses of gravitropic mutants (Supplementary Fig. S2A) using these two systems. Roots of the auxin response factor double-mutant *arf10/arf16* displayed loss of columella cell identity and a disorganised root cap (Wang *et al*., 2005), while *aux1–7* mutant, which carries a mutation in

the auxin transport gene (Bennett *et al*., 1996), and the starchless *pgm1–1* mutants, showed a substantial reduction in gravitropic responses (Kiss *et al*., 1989). When hydrostimulated for 4 h in the air system, gravitropism-deficient mutants (*aux1–7*, *arf10/arf16*, and *pgm1–1*) exhibited significantly higher hydrotropism than wild-type roots (Fig. 1C). The same was true of mutants stimulated for 6 h in the agar-sorbitol system (Fig. 1F). However, the hydrotropism of wild-type roots was similar to that of the mutants when hydrostimulated for 8 h (Fig. 1C). The wild-type (Col-0) and *arf10/arf16* double-mutants showed a similar hydrotropism when hydrostimulated for 12 h, whereas *aux1–7* and *pgm1–1* mutants exhibited significantly higher hydrotropism (Fig. 1F). These results suggest that gravitropism-deficient mutants have increased hydrotropism early during hydrostimulation in OHESs. In both systems, the root angles in the *ahr1* mutants (isolated in VHES systems) were identical to those in wild-type plants (Fig. 1C, 1F). Primary root elongation of these mutants was similar to that in wild-type plants (Supplementary Fig. S2B, C). Collectively, these results suggest that the oblique orientation hydrotropic response of *Arabidopsis* roots in air systems is similar to that in agar-sorbitol systems and that gravitropism-deficient mutants exhibit enhanced hydrotropism in both systems.

Agar-glycerol systems induce vertical orientation hydrotropism in roots

The agar-glycerol system consists of two different media: the top half contains a water stress medium (WSM), and the lower half contains a normal medium (NM) (Saucedo *et al*., 2012; Miao *et al*., 2018). WSM contains 0.5% (v/v) glycerol and 0.1% (w/v) alginic acid (Fig. 2A). First, we employed transgenic plants expressing auxin response reporters (DR5:GFP), an auxin sensor (DII-VENUS) and the principal auxin-influx carrier (AUX1-YFP), and found that the DR5 promoter activity, DII-VENUS signal intensity, and AUX1 expression levels were significantly reduced in the root tips in the presence of the water potential gradient compared to controls (Fig. 2B, 2C). Second, we found that the amount of amyloplast in wild-type roots was substantially decreased under hydrostimulation (Fig. 2D, 2E). Finally, we analysed the response of the primary root to water potential gradients in hydrotropic and gravitropic mutants. *Ahr1* mutants showed remarkable growth toward water-rich substrates compared to wild-type roots, while *miz1* showed reduced growth (Fig. 2F, 2G), in line with previous reports (Saucedo *et al*., 2012; Miao *et al*., 2018). In the agar-glycerol system, *Arabidopsis* root growth was inhibited under hydrostimulation (Fig. 2G),

and wild-type roots were significantly longer than those of gravitropic mutants under hydrostimulation (Fig. 2F, G). These results suggest that the agar-glycerol system can induce vertical orientation hydrotropism and that gravitropism-deficient mutants have decreased hydrotropism under this system.

Sand systems can be used to investigate root hydrotropism in the oblique or vertical orientation

To investigate root hydrotropism under natural conditions, we designed an improved hydrotropism system wherein root system development occurs in the sand in the presence of realistic water potential gradients (Fig. 3A-C). To enhance visualization of distribution of moisture in the raw image of sand in sand system for oblique orientation hydrotropism (SSO) (Fig. 3A), we imaged the sand and enhanced the differences in grey-scale intensity values (Fig. 3B), as previously described (Rellan-Alvarez *et al*., 2015). Thus, differences in grey-scale intensity values corresponded to moisture content gradients (e.g., the water levels in the hydrostimulated chamber of SSO from left to right was 4.1±0.13, 7.79±1.50, 10.10±1.64, and 11.77±1.77). Using this method, we mapped and visualised water levels in the sand (Fig. 3A, 3B). Sand maintained a constantly high water content (approximately 14%) in all zones for 9 days under control conditions; there were no detectable gradients in the water level in the control chamber (Supplementary Table S1). Oblique water content gradients ranging from 4.1% to 11.8% were formed in the hydrostimulated chamber (Supplementary Table S1).

These findings suggest that our sand system accurately simulated oblique water content gradients (Fig. 3C). Therefore, we used it to examine the hydrotropic response of *Arabidopsis* roots in the oblique orientation. The number of lateral roots that emerged on the left side of the primary root was similar to the number that emerged on the right side of the primary root under control conditions (Fig. 3D; Supplementary Fig. S3A). However, the number that emerged on the right (wet) side of the primary root was significantly higher in the presence of water content gradients compared to the number that emerged on the left (dry) side (Fig. 3D). The roots of the Col-0, Ws, and Ler *Arabidopsis* ecotypes showed a similar response (Fig. 3D), indicating that the capacity of the root growth response to oblique water potential gradients is a general phenomenon across genetic backgrounds in *Arabidopsis*. Additionally, the root growth of tomato also exhibited a similar oblique hydrotropic response (Supplementary Fig. S4), while we found no differences in the number of lateral roots on the

wet and dry sides of the primary roots under control or hydrostimulated conditions in *miz1* plants (Fig. 3D; Supplementary Fig. S3A). Furthermore, the ratios between the lateral root length on the wet and dry sides of the chamber were significantly higher in the presence of water content gradients compared to control conditions (Supplementary Fig. S3B), in accordance with previous studies that have used natural drought systems (Iwata *et al*., 2013; Bao *et al*., 2014; Robbins and Dinneny, 2018). *Miz1* plants did not show asymmetry in the length of lateral root on the wet and dry sides of the primary roots under control or hydrostimulated conditions (Supplementary Fig. S3B). These results indicated that in addition to OHESs (air system and agar-sorbitol system), the sand system for oblique orientation hydrotropism (SSO) could be used to investigate oblique orientation hydrotropism.

In nature, roots grow in response to water gradients, and most of the gradients are vertical (Russell, 1977). We developed an improved sand system for vertical orientation hydrotropism (SSV), with water content gradients (ranging from 0.6% to 3.4%) established parallel to the direction of gravity after 9 days of hydrostimulation (Fig. 3E-G). Furthermore, in time-course experiments, we found that the water content gradients were established as early as 5 days after the start of hydrostimulation (Supplementary Table S2). The results further confirmed that this experimental system accurately simulated vertical water content gradients. Therefore, we used this growth system to investigate the hydrotropic response of *Arabidopsis* roots in the vertical orientation. We found that the 5-day hydrostimulation significantly enhanced primary root elongation (Supplementary Fig. S5), and this was closely associated with a steeper water potential gradient (Supplementary Table S2). To investigate if the positive hydrotropic response of roots occurred only in the sand or also in soil microcosms, we quantified the growth of wild-type primary roots in a vertical soil culture system. In this setup, the soil maintained a consistently high water content (were ~36%) in all zones for 9 days (Supplementary Table S3). Compared to control roots, the primary root length of wild-type seedlings was significantly higher in the soil (Supplementary Fig. 6). Because the sand system induced a steeper water potential gradient than real soil (5.7-fold vs. 1.3-fold gradient; Supplementary Table S2 and Supplementary Table S3), and the sand system was easily adjustable, we used it in subsequent experiments.

Under hydrostimulation, the roots of the Ws and Ler *Arabidopsis* ecotypes exhibited a significantly higher hydrotropic elongation than the respective controls, indicating that the

positive hydrotropic response is a general phenomenon across various genetic backgrounds (Fig. 3H; Supplementary Fig. S7A). Moreover, tomato roots showed a similar vertical hydrotropic response under hydrostimulation (Supplementary Fig. S7B, C). In the agar-glycerol system, *ahr1* mutants showed significantly higher primary root elongation than wild-type plants (Fig. 2G); in contrast, in the sand system, primary root elongation in *ahr1* mutants was similar to that in wild-type (Fig. 3H). Hydrostimulation also inhibited the growth of wild-type roots in the agar-glycerol system (Fig. 2G), suggesting that the osmolyte glycerol contained in the agar-glycerol system caused severe osmotic stress. Taken together, these results suggest that the increased primary root elongation is the consequence of an enhanced hydrotropic response because roots continued to grow towards the high-water zone; the sand system may offer a more natural system to study hydrotropism in a vertical orientation.

Hydrostimulation regulates the expression of auxin- and amyloplast-related genes in *miz1* plants

To investigate the molecular expression profile associated with root hydrotropism, we performed RNA sequencing analyses using wild-type (Col-0) and *miz1* roots grown under control (C) and hydrostimulation (H) conditions. We found that hydrostimulation significantly upregulated (>1.5-fold) 365 and 1468 genes in wild-type and *miz1* roots, respectively (Fig. 4A), while 469 and 701 genes were significantly downregulated (<0.5-fold; Fig. 4B). There were 6 DEGs in wild-type roots and 21 DEGs in *miz1* roots that were related to auxin signalling pathway or auxin biosynthesis. For example, *NIT2* (AT3G44300, encoding for a nitrilase), *WAG1* (AT1G53700, involved in wavy root growth), and *YUC3* (AT1G04610, a member of the YUCCA family) were upregulated under hydrostimulation in wild-type roots, while the expression levels of *IAA1* (AT4G14560, indole-3-acetic acid-inducible 1), *SAUR61* (AT1G29420, small auxin upregulated RNA), and *SAUR78* (AT1G72430, small auxin upregulated RNA) were downregulated (Fig. 4C; Supplementary Table S4). Similarly, eight auxin-related genes, including *NIT2*, were upregulated under hydrostimulation in *miz1* roots, while 13 auxin-related genes, such as *IAA14* and *SAUR78* were downregulated (Fig. 4C; Supplementary Table S4). DEGs related to starch (amyloplast) metabolism were also enriched under hydrostimulation (3 DEGs in wild-type roots and 6 DEGs in *miz1* roots). Notably, *AMY3* (AT1G69830, a plastid-localised alpha-amylase) and *LUP1* (AT1G78970, a lupeol synthase 1) were upregulated under hydrostimulation in wild-

type roots, while *BAM9* (AT5G18670, a beta-amylase) was downregulated (Fig. 4C; Supplementary Table S5). *SEX4* (AT3G52180, a plant-specific glucan phosphatase), *SGR5* (AT2G01940, involved in shoot gravitropism) and *SS3* (AT1G11720, a starch synthase) were upregulated under hydrostimulation in *miz1* roots, while *AMY2* (AT1G76130, an alpha-amylase), *BAM3* (AT4G17090, a beta-amylase) and *SGR9* (AT5G02750, involved in shoot gravitropism) were downregulated (Fig. 4C; Supplementary Table S5). These results suggest that hydrostimulation influences the expression of auxin-related and amyloplast-related genes.

Further investigation of changes in the expression of auxin-regulated genes was performed using transgenic plants expressing auxin response reporters (DR5:GFP) in wild-type and *miz1* roots (Fig. 4D; Supplementary Fig. S8A). Under hydrostimulation, the DR5:GFP signal intensity was significantly lower in the root tips of *miz1* plants than wild-type plants (Fig. 4D; Supplementary Fig. S8A), consistent with the RNA sequencing data (Fig. 4C; Supplementary Table S4). In addition, the amounts of amyloplasts were substantially decreased under hydrostimulation, in both wild-type and *miz1* plants (Fig. 4E; Supplementary Fig. S8B).

Role of gravity in oblique orientation hydrotropism in *miz1* roots

MIZ1 is a positive regulator of root hydrotropism in the oblique orientation, and hydrostimulation significantly inhibited auxin responses in the root tips of *miz1* plants (Fig. 4D; Supplementary Fig. S8A). Thus, we examined the genetic link between AUX1 and MIZ1. To generate double-mutant *Arabidopsis* plants, we crossed *miz1* mutant plants with *aux1* mutants. Subsequently, homozygous *miz1/aux1* double-mutant plants were selected on the basis of mutant-specific primers and DNA sequencing (Fig. 5A, B). Compared to wild-type plants, *Miz1*/*aux1* double-mutants exhibited significantly impaired gravitropism (Fig. 5C, D). Next, we examined the hydrotropic response of the *miz1/aux1* double-mutant using different growth systems. In the air system, *Miz1/aux1* double-mutants exhibited a significantly higher hydrotropism than *miz1* single mutants (Fig. 5E), suggesting that the hydrotropism-deficient phenotype of *miz1* roots could be partially rescued via loss of AUX1 function. Given that SSO also induces obliquely oriented water potential gradients, we further assessed the hydrotropic response of the agravitropic double-mutant *miz1/aux1* in SSO. Under hydrostimulation, we observed asymmetry in the lateral root number on wet and dry sides of the primary roots in wild-type plants and *miz1/aux1* double-mutants; however, this

asymmetry was not observed in *miz1* plants (Fig. 5F). Furthermore, the *miz1/aux1* double-mutants exhibited asymmetry in the lateral root length (Supplementary Fig. S9), suggesting that AUX1-regulated gravitropism is involved in the hydrotropic response in *miz1* plants.

Role of gravity in vertical orientation hydrotropism in *miz1* roots

Next, we used the improved sand system for vertical orientation hydrotropism (SSV) and the transgenic plants DR5:GFP and AUX1:YFP to further explore the mechanisms underlying the hydrotropic elongation of primary roots (Fig. 6A). Hydrostimulation enhanced auxin signalling, indicated by the increase in the levels of the auxin response marker DR5:GFP (Fig. 6A, B). Consistently, hydrostimulation treatment significantly increased the protein levels of the auxin importer AUX1-YFP (Fig. 6A, B). In addition, we found that under hydrostimulation, wild-type roots had substantially higher amount of amyloplast compared to controls (Fig. 6C). These results indicate that auxin and amyloplast signalling are required for hydrotropic root elongation in a vertical orientation.

Next, we analysed the root hydrotropism response in gravitropic and hydrotropic mutants (Fig. 6D). Hydrotropic stimulation markedly increased the primary root length (28.5% of control) in wild-type (Col-0) seedlings (Fig. 6D). However, primary root length only increased by 16.7%, 14.7%, and 9.8% under hydrostimulation in *aux1–7*, *arf10/arf1*6, and *pgm1–1* mutants, respectively (Fig. 6D). These results suggest an important role of gravitropism in hydrotropic root elongation. We also used *miz1/aux1* double-mutants to confirm the role of gravity in root hydrotropism in the SSV. The *miz1* mutant exhibited similar amyloplast accumulation to wild-type plants. By contrast, *miz1/aux* double-mutants showed less amyloplast accumulation than wild-type plants under hydrostimulation (Fig. 6E), suggesting that auxin is necessary for hydrostimulation-induced amyloplast accumulation in a vertical orientation. Furthermore, the primary root lengths of *miz1/aux1* double-mutants were shorter than those of wild-type plants (Fig. 6F). Taken together, these results suggest that gravity sensing steers root growth downward, facilitating access to water stored in deeper layers of the sand.

Discussion

Hydrotropic response in *Arabidopsis* under different experimental systems

Soil water in the plant root zone is heterogeneously distributed under natural conditions (Dietrich, 2018). Hydrotropism is the mechanism by which plant roots sense the differences in water potentials in the soil and direct root growth toward water-rich areas (Jaffe *et al*., 1985; Cassab *et al*., 2013; Miao *et al*., 2018). Several successful hydrotropic experimental systems have been established over the years (Takahashi *et al*., 2002; Eapen *et al*., 2003; Saucedo *et al*., 2012). When the primary water source is the rainfall before the growing season, deeper soil layers have higher water content; by simulating this scenario, VHESs facilitate root growth straight down a vertically oriented water gradient column (Fig. 3G). On the other hand, when episodic/occasional rainfall is the primary water source, upper or obliquely oriented soil layers have higher water content (Fig. 1; Fig. 3C); hence, in OHESs, roots elongate preferentially within the upper soil or in obliquely oriented soil layers, leading to characteristic root bending patterns (Lynch, 2013; Feng *et al*., 2016).

However, our results suggest that the same plant genotypes can show distinct root growth patterns in the two hydrotropism systems, owing to the fact that the different systems present different orientations of water potential gradients, with significant variation in space (Figs. 1–3). Under most circumstances, single-orientation hydrotropism systems are used (Supplementary Fig. S1). For instance, air and agar-sorbitol systems only induce oblique water potential gradients. Here, we found that gravitropic mutants exhibited hydrotropic root bending in both systems, highlighting the similarities between the two (Fig. 1C, F). Iwata *et al*. (2013) studied *Arabidopsis* hydrotropism under natural conditions and found that the water gradients were only oblique. When glycerol was used as an osmolyte in the agar-glycerol system (Fig. 2), auxin and amyloplast responses were dramatically decreased in the root tips in the presence of a water potential gradients (Fig. 2C, E), suggesting that osmotic stress inhibits amyloplast and auxin signalling, as previously reported (Takahashi *et al*., 2003; Ponce *et al*., 2010; Xu *et al*., 2013b; Rowe *et al*., 2016). Compared to the respective controls, hydrostimulation inhibited root growth in wild-type and auxin mutants (Fig. 2F, G). Taken together, these results suggest that the presence of the osmolyte glycerol in the growth system not only induces water potential gradients but also induces severe osmotic stress.

Taking these factors into consideration, we designed an improved hydrotropism system that is well suited for studying root hydrotropism in *Arabidopsis* (Fig. 3C, G); we also tested

its utility in the tomato (Supplementary Fig. S4, S7). Importantly, this sand system can be used to investigate root hydrotropism in the oblique (Fig. 3C) or vertical orientation (Fig. 3G). We found that *miz1* plants showed deficient hydrotropism in the oblique orientation under the sand system for oblique orientation hydrotropism (SSO) (Fig. 3D), suggesting that SSO is similar to air system and agar-sorbitol-system (Fig. 1). The sand system for vertical orientation hydrotropism (SSV) significantly promoted vertical root elongation in wild-type (Col-0), *miz1*, and *ahr1* plants (Fig. 6D). By contrast, the agar-glycerol system inhibited vertical root elongation in wild-type and *miz1* plants (Fig. 2F, G), suggesting that the agar-glycerol systems might induce water stress due to the high concentration of glycerol. In addition, given that light influences root development (Xu *et al*., 2013a; Zheng *et al*., 2019), the fact that plant shoots and roots are exposed to illumination in most hydrotropism systems may cause artefacts. In the sand system (Fig. 3), although shoots are illuminated, roots are not exposed to light, simulating the natural environment. Thus, our sand system can reproducibly induce relatively stable and smooth water gradients, and offer a more natural system to study hydrotropism (Fig. 3).

Gravity plays an important role in the MIZ1-regulated root hydrotropism

Under natural conditions, hydrotropic stimulation in the roots occurs simultaneously with gravity sensing (Takahashi *et al*., 2002; Dietrich, 2018). Under these conditions, roots may first judge the location of water, followed by a change in the orientation of the root tip. When the water orientation is oblique to the gravity vector, roots must overcome gravitropism and ultimately initiate root bending toward the obliquely oriented water (Fig. 1). Consistently, previous studies that have used OHESs (air and agar-sorbitol systems) have reported that gravity inhibits root hydrotropism (Krieger *et al*., 2016). We also present evidence on the role of gravity in MIZ1-regulated root hydrotropism. Our transcriptomic data indicated dramatic changes in the expression of multiple genes involved in auxin and amyloplasts response in *miz1* plants during the hydrotropic response (Fig. 4C). Notably, auxin responses were reduced in *miz1* under hydrotropism conditions (Fig. 4D; Supplementary Fig. S8A). In addition, the degradation of amyloplasts in columella cells occurred in both the wild-type and *miz1* mutants upon hydrostimulation (Fig. 4E; Supplementary Fig. S8B). These results imply that auxin and amyloplast responses may be important for the hydrotropic mutant *miz1*. Because amyloplasts in root columella cells are

required for gravity sensing, amyloplast degradation is thought to play an important role in negating gravisensing and might regulate hydrotropism-dependent root growth (Takahashi *et al*., 2003). Furthermore, genetically gravitropism-modified *miz1/aux1* double-mutants exhibited hydrotropic bending due to gravitropism impairments (Fig. 5). Taken together, these results pinpoint an antagonistic relationship between hydrotropism and gravitropism, and indicate that in the absence of gravitropism (loss of AUX1 function), the response to lateral water potential gradients in *miz1* plants is partially restored.

In our sand system, oblique orientation hydrotropism was similar to hydropatterning (Fig. 3C). Previous studies have indicated that primary roots exhibit obliquely oriented hydrotropism in both air and agar-sorbitol systems (Fig. 1), while during hydropatterning, lateral roots emerge toward water-rich areas (Orosa-Puente *et al*. 2018). The primary roots of *miz1* mutants did not show obliquely oriented hydrotropism in air or agar-sorbitol systems (Fig. 1), and the lateral roots of *miz1* mutants did not emerge toward water-rich areas in the soil (Iwata *et al*., 2013) or in our sand system (Fig. 3D); these findings suggest that oblique orientation hydrotropism was similar to hydropatterning. Importantly, *miz1* mutants not only exhibited oblique orientation hydrotropism deficiencies in primary roots but also showed hydropatterning deficiencies in lateral roots (Fig. 1; Fig. 3D). In addition, wild-type plants exhibited oblique orientation hydrotropism in primary roots and hydropatterning in lateral roots, further supporting that oblique orientation hydrotropism is similar to hydropatterning. Given that primary and lateral roots make up the majority of the plant root system (Malamy, 2005), obliquely oriented hydrotropism and hydropatterning in roots may be important for enhancing the growth of terrestrial plants when water availability is limited.

In response to drought, plants increase the root-to-shoot ratio, by growing longer roots and inhibiting shoot growth (van der Weele *et al*., 2000; Sharp *et al*., 2004; Sharp and LeNoble, 2002; Uga *et al*., 2013). Polyethylene glycol (PEG) is commonly added to the medium to reduce water potential (Rowe *et al*., 2016), and there is probably less of a gradient in the system. In addition, soil drying experiments (pot-grown plants and plants grown in the field) are typically employed to measure certain aspects of plant growth, survival, and water status (Verslues *et al*., 2006; Dodd *et al*., 2008a, b). Water gradients in such experiments are affected by pot dimensions/irrigation placement (Dodd *et al*., 2011; Puértolas *et al*., 2013). Our sand system for vertical orientation hydrotropism (SSV) is similar to soil drying experiments in that vertical water content gradients were significantly established (Fig. 3G).

For the measurement of vertical orientation hydrotropism, the agar-glycerol system can induce the vertical water-potential gradients from low to high (Fig. 2A). Then, the water content gradients in the sand system can be compared to the water-potential gradients of the agar-glycerol system: the lower water-content in the top of the sand system reflects the lower water-potential, and the higher water content in the bottom of the sand system reflects the higher water-potential (Fig. 3G); Thus, based on establishing water contents in sand or soil, water content gradients in the sand system or soil drying experiments can also reflect the water-potential gradients from low to high (Dodd *et al*., 2006; Dodd *et al*., 2008b; Puértolas *et al*., 2013). In addition, compared to the agar-glycerol system, the sand system or soil drying experiments is more close to the natural conditions. Although amyloplast and auxin responses were enhanced upon hydrostimulation in the SSV system (Fig. 6A-C), these responses were reduced in the agar-glycerol system (Fig. 2B-E), further supporting that the sand system is superior to the agar-glycerol system in providing stable vertically oriented water gradients. Furthermore, hydrotropic stimulation in the SSV markedly increased the primary root length in wild-type seedlings, whereas agravitropic mutants were unable to reach the higher water potential present in deeper wet sand layers (Fig. 6D, F). This result is in agreement with previous studies showing that drought conditions induce steeper roots, aiding water uptake (Rellan-Alvarez *et al*., 2015; Uga *et al*., 2013; Lynch, 2013). Moreover, *miz1*/*aux1* double-mutants showed attenuated root elongation towards the water in a vertical orientation (Fig. 6F), suggesting that gravity is essential for the vertically oriented hydrotropism of roots. These findings also indicate that plants with an increased root growth angle in response to gravity stimulation will be better able to tap into deep water resources typically present in deeper soil layers, ensuring adequate water supply and thereby reducing the need for irrigation (Mingo *et al*., 2004; Eapen *et al*., 2017; Robbins and Dinneny, 2018).

In conclusion, we present a sand system that simulates natural conditions more accurately than traditional systems, with dynamic water potential gradients established not only in the oblique orientation but also in the vertical orientation. This system is, therefore, ideal for the study of root hydrotropic responses. We also provide evidence that gravity plays an essential role in the MIZ1-regulated root hydrotropism (Fig. 7). When the water orientation is oblique to the gravity vector, the gravity vector hinders root bending and the acquisition of obliquely oriented water. Wild-type and *miz1/aux1* double-mutant plants show hydrotropic root bending, whereas *miz1* mutants do not show hydrotropic root bending (Fig.

7A). On the other hand, when water orientation is parallel to the gravity vector, gravity sensing promotes root growth in a straight downward direction to allow for the capture of vertically oriented water. Wild-type and *miz1* plants show root elongation towards the water in a vertical orientation, whereas *miz1/aux1* double-mutants do not show root elongation towards the water in a vertical orientation (Fig. 7B). Overall, based on comparative analyses using various hydrotropic experimental systems, we propose that gravity impedes roots' search for obliquely oriented water while facilitating roots' search for vertically oriented water. Understanding the mechanisms of interaction between hydrotropism and gravitropism is pivotal to our understanding of the rooting patterns of plants under natural conditions, as efforts intensify to improve the crop water uptake to meet the increasing demands for food under the rapidly changing climate conditions.

Data availability

The RNA sequencing data generated in this study have been deposited in NCBI (https://www.ncbi.nlm.nih.gov/sra/PRJNA641259), and SRA (Sequence Read Archive) accession is PRJNA641259.

Acknowledgements

We thank Prof. Gladys I. Cassab (Universidad Nacional Autónoma de México) for providing the *ahr1* seeds. We are grateful for the financial support from the National Key R&D Program of China (2017YFE0118100 and 2018YFD0200302), the National Natural Science Foundation of China (31872169, 31761130073, 31422047), and a Newton Advanced Fellowship (NSFC-RS: NA160430).

Author contributions

W.X., Y.L. and W.Y. planned and designed the research. L.L., H.D., and X.D. performed experiments and analysed the data. Y.L., W.X., W.Y., J.Z., R.M., F.B., H.K. and C.L. discussed and wrote the manuscript. W.X. agrees to serve as the author responsible for scientific communication.

References

Band LR, Wells DM, Larrieu A, *et al.* 2012. Root gravitropism is regulated by a transient lateral auxin gradient controlled by a tipping-point mechanism. Proceedings of the National Academy of Sciences, USA **109,** 4668-4673.

Bao Y, Aggarwal P, Robbins NE, *et al.* 2014. Plant roots use a patterning mechanism to position lateral root branches toward available water. Proceedings of the National Academy of Sciences, USA **111,** 9319-9324.

Bennett MJ, Marchant A, Green HG, May ST, Ward SP, Millner PA, Walker AR, Schulz B, Feldmann KA. 1996. Arabidopsis AUX1 gene: a permease-like regulator of root gravitropism. Science **273,** 948-950.

Cassab GI, Eapen D, Campos ME. 2013. Root hydrotropism: an update. American Journal of Botany **100,** 14-24.

Chang JK, Li XP, Fu WH, *et al.* 2019. Asymmetric distribution of cytokinins determines root hydrotropism in Arabidopsis thaliana. Cell Research **29,** 984-993.

Claeys H, Van Landeghem S, Dubois M, Maleux K, Inze D. 2014. What Is Stress? Dose-Response Effects in Commonly Used in Vitro Stress Assays. Plant Physiology **165,** 519-527.

Cole ES, Mahall BE. 2006. A test for hydrotropic behavior by roots of two coastal dune shrubs. New Phytologist **172,** 358-368.

Darwin C, Darwin F. 1880. The Power of Movement in Plants. London: John Murray.

Dietrich D. 2018. Hydrotropism: how roots search for water. Journal of Experimental Botany **69,** 2759-2771.

Dietrich D, Pang L, Kobayashi A, *et al.* 2017. Root hydrotropism is controlled via a cortex-specific growth mechanism. Nature Plants **3,** 17057.

Dodd IC, Egea G, Davies WJ. 2008a. Abscisic acid signalling when soil moisture is heterogeneous: decreased photoperiod sap flow from drying roots limits abscisic acid export to the shoots. Plant Cell and Environment **31,** 1263-1274.

Dodd IC, Egea G, Davies WJ. 2008b. Accounting for sap flow from different parts of the root system improves the prediction of xylem ABA concentration in plants grown with heterogeneous soil moisture. Journal of Experimental Botany **59,** 4083-4093.

Dodd IC, Theobald JC, Bacon MA, Davies WJ. 2006. Alternation of wet and dry sides during partial rootzone drying irrigation alters root-to-shoot signalling of abscisic acid. Functional Plant Biology **33,** 1081-1089.

Dodd IC, Whalley WR, Ober ES, Parry MAJ. 2011. Genetic and management approaches to boost UK wheat yields by ameliorating water deficits. Journal of Experimental Botany **62,** 5241-5248.

Eapen D, Barroso ML, Campos ME, Ponce G, Corkidi G, Dubrovsky JG, Cassab GI. 2003. A no hydrotropic response root mutant that responds positively to gravitropism in Arabidopsis. Plant Physiology **131,** 536-546.

Eapen D, Barroso ML, Ponce G, Campos ME, Cassab GI. 2005. Hydrotropism: root growth responses to water. Trends in Plant Science **10,** 44-50.

Eapen D, Martinez-Guadarrama J, Hernandez-Bruno O, Flores L, Nieto-Sotelo J, Cassab GI. 2017. Synergy between root hydrotropic response and root biomass in maize (Zea mays L.) enhances drought avoidance. Plant Science **265,** 87-99.

Eysholdt-Derzso E, Sauter M. 2017. Root Bending Is Antagonistically Affected by Hypoxia and ERF-Mediated Transcription via Auxin Signaling. Plant Physiology **175,** 412-423.

Feng W, Lindner H, Robbins NE, Dinneny JR. 2016. Growing Out of Stress: The Role of Cell- and Organ-Scale Growth Control in Plant Water-Stress Responses. Plant Cell **28,** 1769-1782.

Hooker HD. 1915. Hydrotropism in roots of *Lupinus albus*. Annals of Botany **29,** 265-283.

Iwata S, Miyazawa Y, Fujii N, Takahashi H. 2013. MIZ1-regulated hydrotropism functions in the growth and survival of Arabidopsis thaliana under natural conditions. Annals of Botany **112,** 103-114.

Jaffe MJ, Takahashi H, Biro RL. 1985. A pea mutant for the study of hydrotropism in roots. Science **230,** 445-447.

Kaneyasu T, Kobayashi A, Nakayama M, Fujii N, Takahashi H, Miyazawa Y. 2007. Auxin response, but not its polar transport, plays a role in hydrotropism of Arabidopsis roots. Journal of Experimental Botany **58,** 1143-1150.

Kiss JZ. 2007. Where's the water? Hydrotropism in plants. Proceedings of the National Academy of Sciences, USA **104,** 4247-4248.

Kiss JZ, Hertel R, Sack FD. 1989. Amyloplasts are necessary for full gravitropic sensitivity in roots of Arabidopsis thaliana. Planta **177,** 198-206.

Kobayashi A, Takahashi A, Kakimoto Y, Miyazawa Y, Fujii N, Higashitani A, Takahashi H. 2007. A gene essential for hydrotropism in roots. Proceedings of the National Academy of Sciences, USA **104,** 4724-4729.

Krieger G, Shkolnik D, Miller G, Fromm H. 2016. Reactive Oxygen Species Tune Root Tropic Responses. Plant Physiology **172,** 1209-1220.

Li BH, Li Q, Su YH, Chen H, Xiong LM, Mi GH, Kronzucker HJ, Shi WM. 2011. Shoot-supplied ammonium targets the root auxin influx carrier AUX1 and inhibits lateral root emergence in Arabidopsis. Plant Cell and Environment **34,** 933-946.

Lynch JP. 2013. Steep, cheap and deep: an ideotype to optimize water and N acquisition by maize root systems. Annals of Botany **112,** 347-357.

Malamy JE. 2005. Intrinsic and environmental response pathways that regulate root system architecture. Plant Cell and Environment **28,** 67-77.

Miao R, Wang M, Yuan W, Ren Y, Li Y, Zhang N, Zhang JH, Kronzucker HJ, Xu WF. 2018. Comparative Analysis of Arabidopsis Ecotypes Reveals a Role for Brassinosteroids in Root Hydrotropism. Plant Physiology **176,** 2720-2736.

Mingo DM, Theobald JC, Bacon MA, Davies WJ, Dodd IC. 2004. Biomass allocation in tomato (Lycopersicon esculentum) plants grown under partial rootzone drying: enhancement of root growth. Functional Plant Biology **31,** 971-978.

Miyazawa Y, Takahashi A, Kobayashi A, Kaneyasu T, Fujii N, Takahashi H. 2009. GNOM-Mediated Vesicular Trafficking Plays an Essential Role in Hydrotropism of Arabidopsis Roots. Plant Physiology **149,** 835-840.

Miyazawa Y, Yamazaki T, Moriwaki T, Takahashi H. 2011. Root Tropism: Its Mechanism and Possible Functions in Drought Avoidance. Plant Responses to Drought and Salinity Stress: Developments in a Post-Genomic Era **57,** 349-375.

Morohashi K, Okamoto M, Yamazaki C, *et al.* 2017. Gravitropism interferes with hydrotropism via counteracting auxin dynamics in cucumber roots: clinorotation and spaceflight experiments. New Phytologist **215,** 1476-1489.

Munne-Bosch S, Alegre L. 2002. Plant aging increases oxidative stress in chloroplasts. Planta **214,** 608-615.

Muthert LWF, Izzo LG, van Zanten M, Aronne G. 2020. Root Tropisms: Investigations on Earth and in Space to Unravel Plant Growth Direction. Frontiers in Plant Science **10,** 1807.

Noriega-Calixto L, Campos ME, Cassab GI. 2019. A method for rapid analysis of the root hydrotropic response in Arabidopsis thaliana. Biotechniques **66,** 154-158.

Orosa-Puente B, Leftley N, von Wangenheim D, *et al*. 2018. Root branching toward water involves posttranslational modification of transcription factor ARF7. Science **362,** 1407-1410.

Ponce G, Corkidi G, Eapen D, Lledias F, Cardenas L, Cassab G. 2017. Root hydrotropism and thigmotropism in Arabidopsis thaliana are differentially controlled by redox status. Plant Signaling and Behavior **12,** e1305536.

Ponce G, Rasgado FA, Cassab GI. 2008. Roles of amyloplasts and water deficit in root tropisms. Plant Cell and Environment **31,** 205-217.

Puértolas J, Alcobendas R, Alarcon JJ, Dodd IC. 2013. Long-distance abscisic acid signalling under different vertical soil moisture gradients depends on bulk root water potential and average soil water content in the root zone. Plant Cell and Environment **36,** 1465-1475.

Rellan-Alvarez R, Lobet G, Lindner H, *et al*. 2015. GLO-Roots: an imaging platform enabling multidimensional characterization of soil-grown root systems. eLife **4,** e07597.

Robbins NE, Dinneny JR. 2018. Growth is required for perception of water availability to pattern root branches in plants. Proceedings of the National Academy of Sciences, USA **115,** E822-E831.

Rowe JH, Topping JF, Liu JL, Lindsey K. 2016. Abscisic acid regulates root growth under osmotic stress conditions via an interacting hormonal network with cytokinin, ethylene and auxin. New Phytologist **211,** 225-239.

Russell RS. 1977. Plant root systems: their function and interaction with the soil. London: McGraw-Hill.

Sachs J. 1872. Ablenkung der Wurzel von ihrer normalen Wachsthumsrichtung durch feuchte Koerper. In: **Sachs J,** ed. Arbeitendes Botanischen Institus in Wuerzburg. Leipzig: Wilhelm Engelmann, 209-222.

Saucedo M, Ponce G, Campos ME, Eapen D, Garcia E, Lujan R, Sanchez Y, Cassab GI. 2012. An altered hydrotropic response (*ahr1*) mutant of Arabidopsis recovers root hydrotropism with cytokinin. Journal of Experimental Botany **63,** 3587-3601.

Sharp RE, LeNoble ME. 2002. ABA, ethylene and the control of shoot and root growth under water stress. Journal of Experimental Botany **53,** 33-37.

Sharp RE, Poroyko V, Hejlek LG, Spollen WG, Springer GK, Bohnert HJ, Nguyen HT. 2004. Root growth maintenance during water deficits: physiology to functional genomics. Journal of Experimental Botany **55,** 2343-2351.

Shkolnik D, Krieger G, Nuriel R, Fromm H. 2016. Hydrotropism: root bending does not require auxin redistribution. Molecular Plant **9,** 757-759.

Shkolnik D, Nuriel R, Bonza MC, Costa A, Fromm H. 2018. MIZ1 regulates ECA1 to generate a slow, long-distance phloem-transmitted Ca^{2+} signal essential for root water tracking in Arabidopsis. Proceedings of the National Academy of Sciences, USA **115,** 8031-8036.

Silva-Navas J, Moreno-Risueno MA, Manzano C, Tellez-Robledo B, Navarro-Neila S, Carrasco V, Pollmann S, Gallego FJ, del Pozo JC. 2016. Flavonols Mediate Root Phototropism and Growth through Regulation of Proliferation-to-Differentiation Transition. Plant Cell **28,** 1372-1387.

Stinemetz C, Takahashi H, Suge H. 1996. Characterization of hydrotropism: the timing of perception and signal movement from the root cap in the agravitropic pea mutant ageotropum. Plant and Cell Physiology **37,** 800-805.

Su SH, Gibbs NM, Jancewicz AL, Masson PH. 2017. Molecular Mechanisms of Root Gravitropism. Current Biology **27,** R964-R972.

Takahashi H, Miyazawa Y, Fujii N. 2009. Hormonal interactions during root tropic growth: hydrotropism versus gravitropism. Plant Molecular Biology **69,** 489-502.

Takahashi H, Mizuno H, Kamada M, *et al*. 1999. A spaceflight experiment for the study of gravimorphogenesis and hydrotropism in cucumber seedlings. Journal of Plant Research **112,** 497-505.

Takahashi H, Scott TK. 1991. Hydrotropism and its interaction with gravitropism in maize roots. Plant Physiology **96,** 558-564.

Takahashi N, Goto N, Okada K, Takahashi H. 2002. Hydrotropism in abscisic acid, wavy, and gravitropic mutants of Arabidopsis thaliana. Planta **216,** 203-211.

Takahashi N, Yamazaki Y, Kobayashi A, Higashitani A, Takahashi H. 2003. Hydrotropism interacts with gravitropism by degrading amyloplasts in seedling roots of Arabidopsis and radish. Plant Physiology **132,** 805-810.

Uga Y, Sugimoto K, Ogawa S, *et al*. 2013. Control of root system architecture by DEEPER ROOTING 1 increases rice yield under drought conditions. Nature Genetics **45,** 1097-1102.

van der Weele CM, Spollen WG, Sharp RE, Baskin TI. 2000. Growth of Arabidopsis thaliana seedlings under water deficit studied by control of water potential in nutrient-agar media. Journal of Experimental Botany **51,** 1555-1562.

Vandenbrink JP, Kiss JZ. 2019. Plant responses to gravity. Seminars in Cell and Developmental Biology **92,** 122-125.

Verslues PE, Agarwal M, Katiyar-Agarwal S, Zhu J, Zhu JK. 2006. Methods and concepts in quantifying resistance to drought, salt and freezing, abiotic stresses that affect plant water status. Plant Journal **45,** 523-529.

Wang JW, Wang LJ, Mao YB, Cai WJ, Xue HW, Chen XY. 2005. Control of root cap formation by microRNA-targeted auxin response factors in Arabidopsis. Plant Cell **17,** 2204-2216.

Xu WF, Ding GC, Yokawa K, Baluska F, Li QF, Liu YG, Shi WM, Liang JS, Zhang JH. 2013a. An improved agar-plate method for studying root growth and response of Arabidopsis thaliana. Scientific Report **3,** 1273.

Xu WF, Jia LG, Shi WM, Liang JS, Zhou F, Li QF, Zhang JH. 2013b. Abscisic acid accumulation modulates auxin transport in the root tip to enhance proton secretion for maintaining root growth under moderate water stress. New Phytologist **197,** 139-150.

Zheng Z, Wang Z, Wang XY, Liu D. 2019. Blue Light-Triggered Chemical Reactions Underlie Phosphate Deficiency-Induced Inhibition of Root Elongation of Arabidopsis Seedlings Grown in Petri Dishes. Molecular Plant **12,** 1515-1523.

Zhu JK. 2016. Abiotic Stress Signaling and Responses in Plants. Cell **167,** 313-324.

Figure legends

Fig. 1. Hydrotropic responses in mutants and wild-type *Arabidopsis* in the oblique orientation using air or agar-sorbitol systems.

(A) Diagram illustrating the air system for testing hydrotropism. The system is described in detail in Methods and previous studies.

(**B**) Representative micrographs of mutant and wild-type *Arabidopsis* seedlings hydrostimulated for 4 h in the air system. All roots were photographed using a stereomicroscope 4 h after the start of hydrostimulation. Scale bar = 1 mm. The following mutants were analysed: no-hydrotropic mutant *miz1*, altered hydrotropic response mutant *ahr1*, three gravitropism-deficient mutants (the auxin response factor double-mutant *arf10/arf16* displaying loss of columella cell identity and a disorganised root cap, *aux1–7* mutant carrying a mutation in the auxin transport gene and the starchless *pgm1–1* mutant).

(**C**) Hydrotropic bending after 4 h or 8 h incubation in the air system.

(**D**) Diagram illustrating the agar-sorbitol system for testing hydrotropism. The system is described in detail in Methods and previous studies.

(**E**) Representative images of mutant and wild-type *Arabidopsis* roots hydrostimulated for 6 h in the agar-sorbitol system. Scale bar = 2 mm.

(**F**) Hydrotropic bending of mutant and wild-type roots after 6 h or 12 h of growth under control (half-strength MS medium) or hydrostimulation (half-strength MS medium + 400 mM sorbitol) conditions.

Data in C and F are presented as means ± SEs of three independent biological replicates; different letters denote significant differences ($P < 0.05$, Duncan's test).

Fig. 2. Hydrotropic responses in mutants and wild-type *Arabidopsis* in vertical orientation using the agar-glycerol system.

(**A**) Diagram illustrating the agar-glycerol system for testing hydrotropism. The system is described in detail in Methods.

(**B**) DR5:GFP, DII-VENUS and AUX1pro:AUX1-YFP signals after four days of growth under control (1/2 MS) or hydrostimulation. Scale bar = 20 µm.

(**C**) Quantification of fluorescence intensities in the roots of plants described in B.

(**D-E**) Representative micrographs (D) and quantification (E) of amyloplasts in wild-type (Col-0) plants grown in the agar-glycerol system. Scale bar = 20 µm.

(**F**) Representative images of mutant and wild-type seedlings under hydrostimulation. Scale bar = 5 mm.

(**G**) Primary root length of mutant and wild-type seedlings. Primary root length was defined as the growth of roots after transferring into a new medium (Control or AGS).

Data in C and G are presented as means ± SEs of three independent biological replicates; asterisks denote significant differences ($P < 0.05$, Duncan's test). Data in E are presented as means ± SEs of three independent biological replicates; asterisks denote significant differences ($P < 0.05$, Student's t-test).

Fig. 3. Oblique orientation hydrotropism (A-D) and vertical orientation hydrotropism (E-H) in mutant and wild-type *Arabidopsis* grown in the sand system.

(**A**) Representative raw sand images showing the sand system for oblique orientation hydrotropism (SSO). After hydrostimulation, the lid covering the control (top) and plastic film/sterile gauze covering the hydrostimulated chamber (bottom) were removed, and raw sand images were taken using a digital Nikon camera D7100. Scale bars = 1.0 cm. Water content was calculated as (fresh weight–dry weight)/fresh weight. The system is described in detail in Methods.

(B) Water distribution in the control and SSO. Pseudo-coloured images (Fig. 3B) were generated from the raw images (Fig. 3A) to show water distribution in the sand. Differences in grey-scale intensity values were enhanced using a 16-colour LUT. Scale bars = 1.0 cm

(**C**) Diagram illustrating the control and SSO. For a detailed description of the assays see Methods.

(**D**) Hydrotropic response of *Arabidopsis* ecotypes and *miz1* mutant in control and SSO.

(E) Representative raw sand images showing the sand system for vertical orientation hydrotropism (SSV). After hydrostimulation, cups were carefully cut lengthwise, and raw sand images were taken using a digital Nikon camera D7100. Scale bars = 0.85 cm. Water content was calculated as (fresh weight–dry weight)/fresh weight. The system is described in detail in Methods.

(**F**) Water distribution in the control and sand system for SSV. Pseudo-coloured images (Fig. 3F) were generated from the raw images (Fig. 3E) to show water distribution in the sand. Differences in grey-scale intensity values were enhanced using 16-colour LUT. Scale bars = 0.85 cm

(**G**) Diagram illustrating the control and SSV. For a detailed description of the assays see Methods.

(**H**) Primary root length of *Arabidopsis* ecotypes and *ahr1* mutant in control and SSV.

Data in D and H are presented as means ± SEs of three independent biological replicates; different letters denote significant differences ($P < 0.05$, Duncan's test).

Fig. 4. The role of auxin- and amyloplast-related pathways in the roots of *miz1* mutant during the hydrotropic response.

(**A, B**) Venn diagrams summarising the changes in gene expression in *miz1* roots. RNA sequencing analyses were performed with wild-type and *miz1* roots, and the numbers of upregulated (>1.5-fold, A) or downregulated (<0.5-fold, B) genes in the *miz1* mutant under control (C) or hydrostimulated (H) conditions are shown.

(**C**) Changes in the expression levels of auxin- and amyloplast-related genes in *miz1* roots. The means and SD were calculated using the RNA sequencing data from three biological replicates.

(**D**) DR5:GFP signal in wild-type (Col-0) and *miz1* roots under control (C) or hydrostimulated (H) conditions.

(**E**) The amount of amyloplasts in wild-type (Col-0) and *miz1* roots under control (C) or hydrostimulated (H) conditions.

In C, $^{**}P < 0.01$ and $^{*}P < 0.05$ indicate significant differences in Col-0 or *miz1* mutant roots (two-tailed Student's *t*-test). Data in D and E are presented as means ± SEs of three independent biological replicates; different letters denote significant differences ($P < 0.05$, Duncan's test).

Fig. 5. The role of gravity in oblique orientation hydrotropism in *miz1* roots.

(**A**) The homozygous *miz1* mutant was identified using three mutant-specific primers (LBb1.3+LP+RP).

(**B**) The DNA sequences of wild-type and *miz1*/*aux1* double-mutant. *mutation at nucleotide 459.

(**C**) Representative phenotypes of 6-day-old mutant and wild-type *Arabidopsis* seedlings. Scale bar = 0.5 cm.

(**D**) Root gravitropic bending kinetics in mutant and wild-type plants.

(**E**) Root hydrotropic bending in mutant and wild-type plants hydrostimulated for 8 h in the air system.

(**F**) Hydrotropic response in mutant and wild-type roots grown in the sand system for SSO.

Data in D, E and F, are presented as means ± SEs of three independent biological replicates; different letters denote significant differences ($P < 0.05$, Duncan's test).

Fig. 6. Role of gravity in vertical orientation hydrotropism in *miz1* roots.

(**A**) DR5:GFP and AUX1pro:AUX1-GFP fluorescent signals in root tips of plants grown in the sand system for vertical orientation hydrotropism (SSV) were detected by confocal microscopy. Scale bars = 20 μm.

(**B**) Quantification of fluorescence intensities in the root tip cells shown in A.

(**C**) Representative micrographs and quantification of amyloplasts in wild-type (Col-0) columella cells in the sand system for SSV.

(**D**) Relative primary root length in wild-type and mutant plants in the sand system for SSV. The primary root length of all plants under control conditions was considered 100%; the relative primary root length was calculated from the primary root length relative to the displacement of primary root apex for the duration of hydrostimulation.

(**E**) Representative micrographs and quantification of amyloplasts in wild-type (Col-0) and mutant columella cells upon hydrostimulation in the sand system for SSV.

(**F**) Primary root length in wild-type and mutant plants in the sand system for SSV.

In A-D, plants were grown under humidity-saturated conditions for 9 days and an additional 7 days under either humidity-saturated or hydrostimulated conditions. In E and F, plants were grown under humidity-saturated conditions for 5 days and an additional 7 days under either humidity-saturated or hydrostimulated conditions. Data in B and C are presented as means ± SEs of three independent biological replicates; asterisks denote significant differences ($P < 0.05$, Student's t-test). Data in D, E and F, are presented as means ± SEs of three independent biological replicates; different letters denote significant differences ($P < 0.05$, Duncan's test).

Fig. 7. Proposed model illustrating the divergent roles of gravity in root hydrotropism.

(**A**) When water orientation is oblique to the gravity vector, the gravity vector hinders root bending. In the presence of obliquely oriented water, wild-type and *miz1/aux1* double-mutant plants show hydrotropic root bending, whereas *miz1* mutants do not show hydrotropic root bending.

(**B**) When water orientation is parallel to the gravity vector, gravity sensing promotes root growth in a straight downward direction allowing for the capture of vertically oriented water. Under these conditions, wild-type and *miz1* plants show root elongation towards the water in a vertical orientation, whereas *miz1/aux1* double-mutants do not show root elongation towards the water in a vertical orientation.

Figure 1

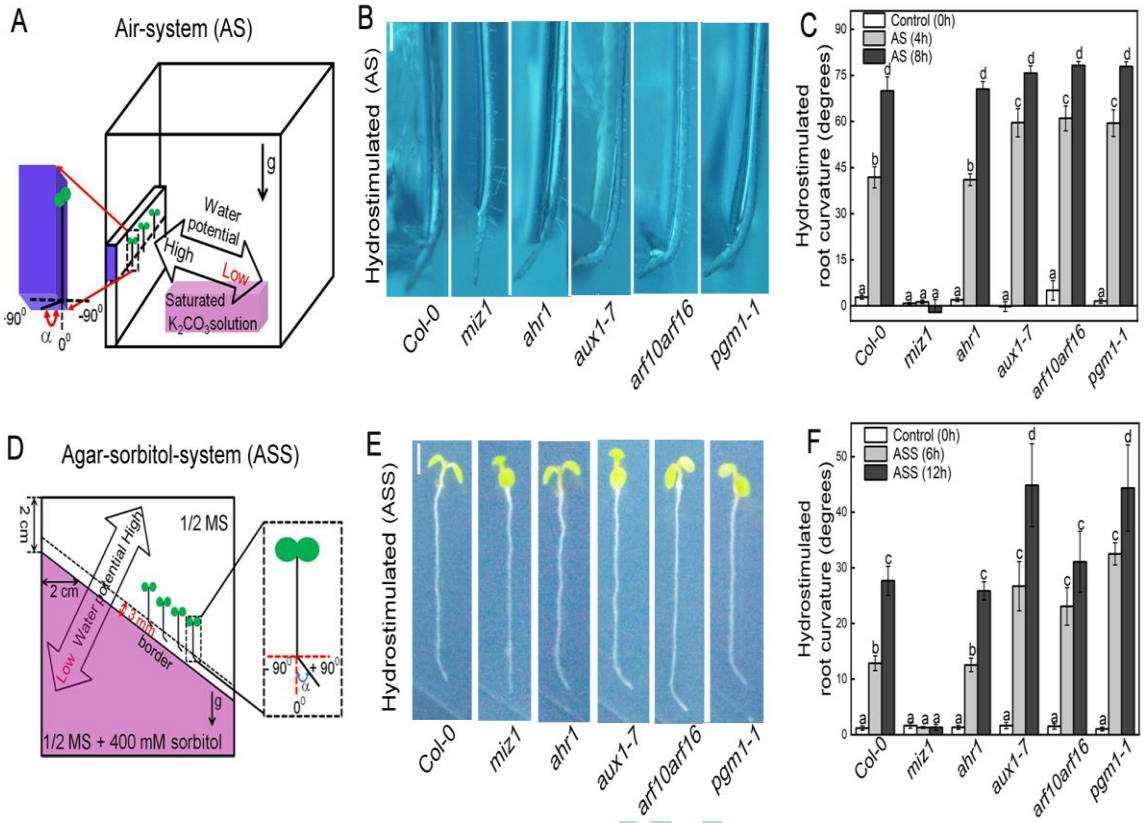

Figure 2

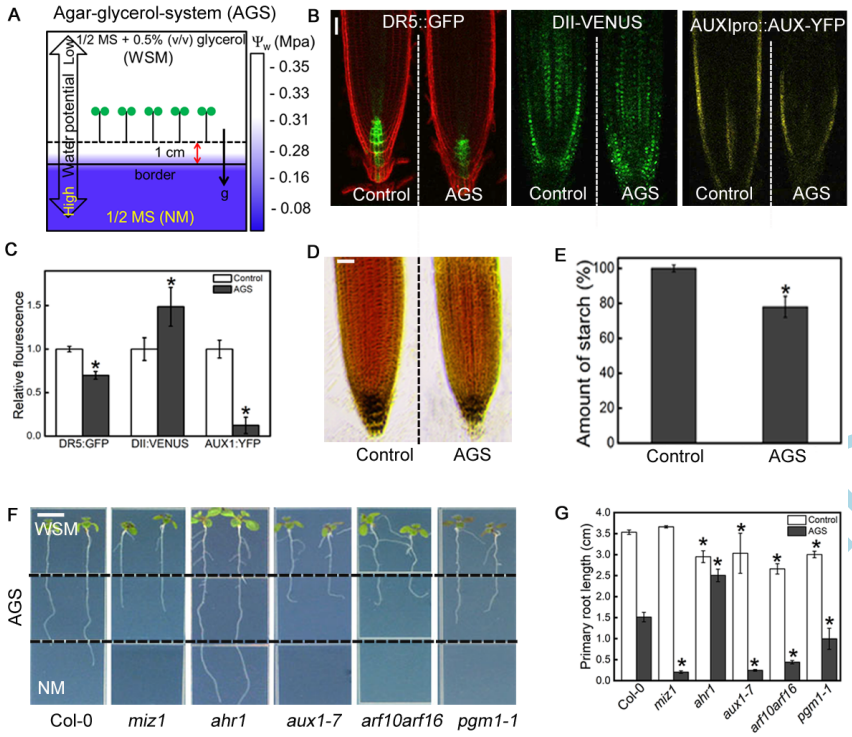

Figure 3

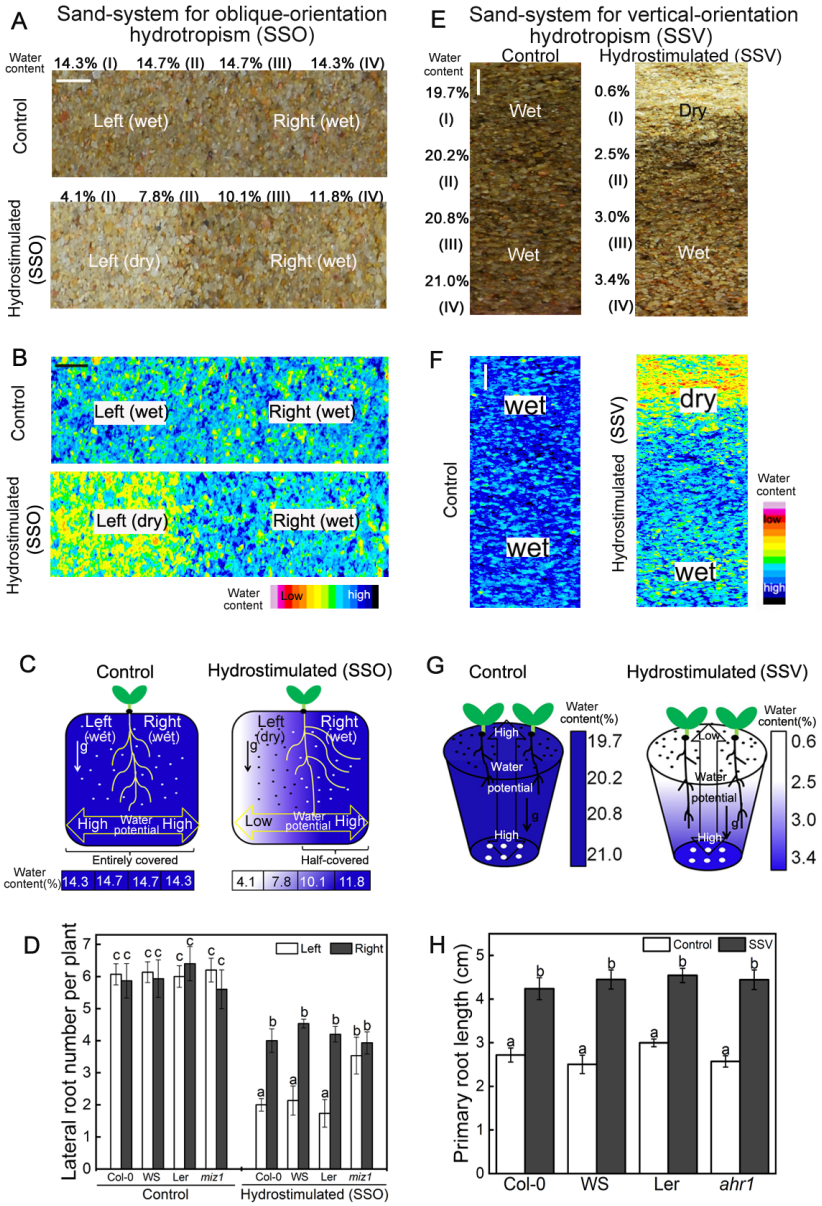

Figure 4

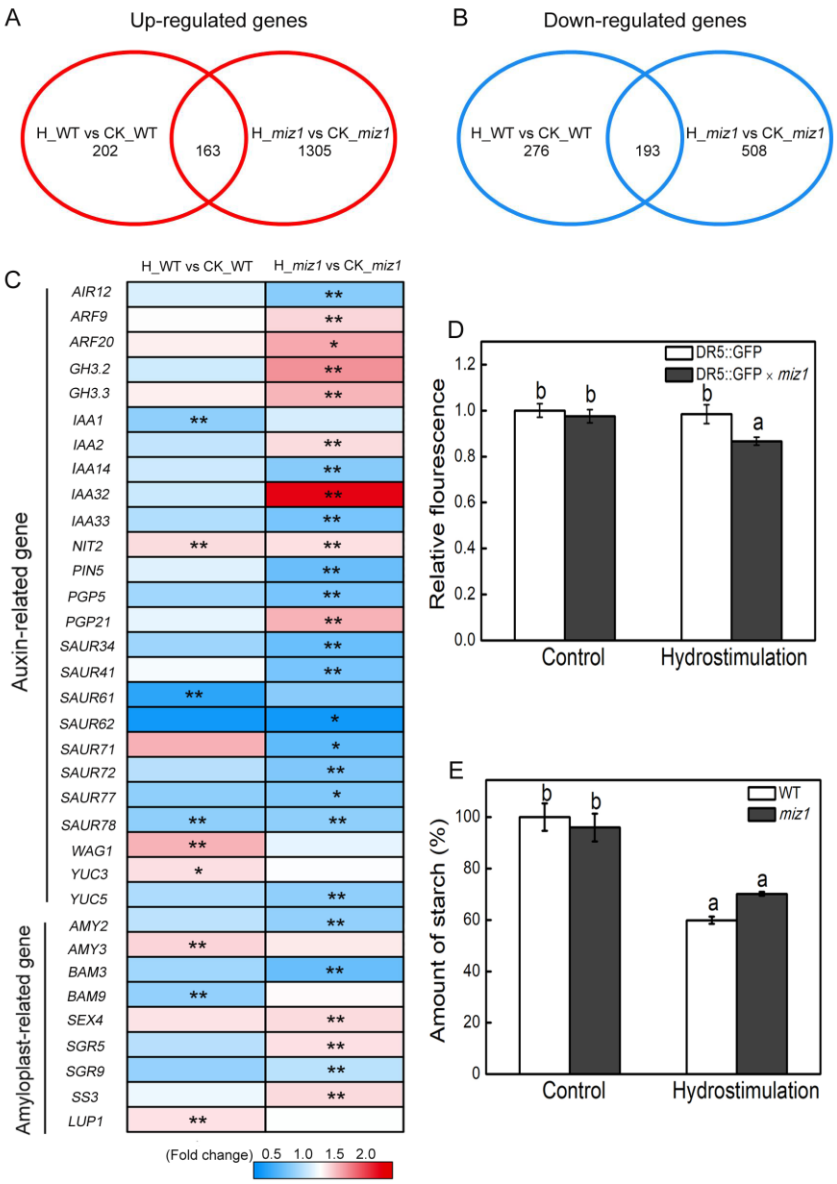

Figure 5

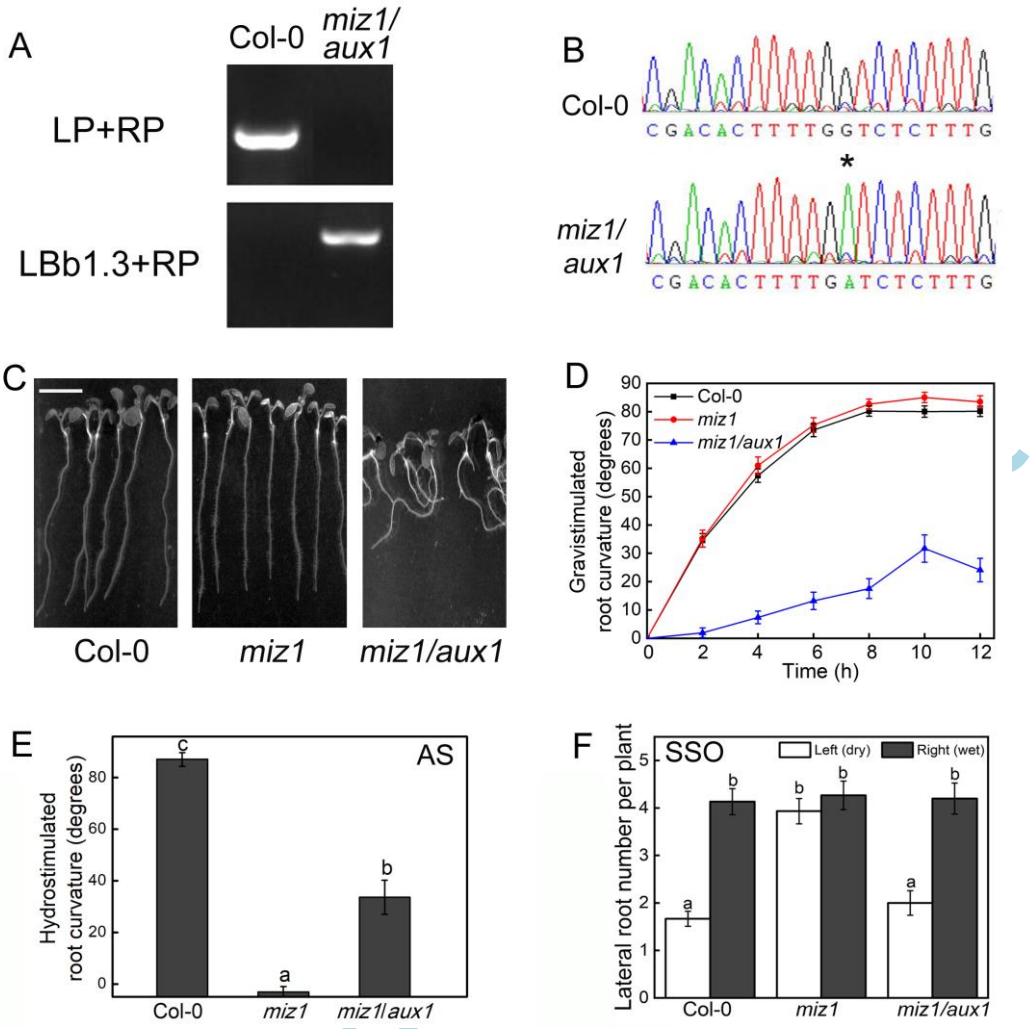

Figure 6

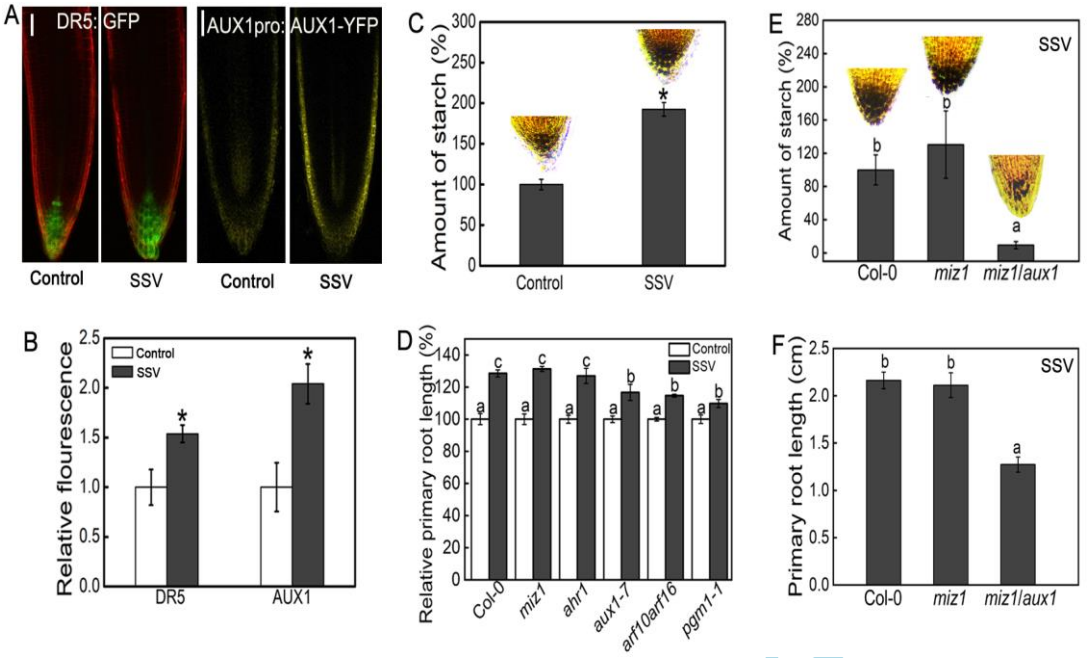

Figure 7